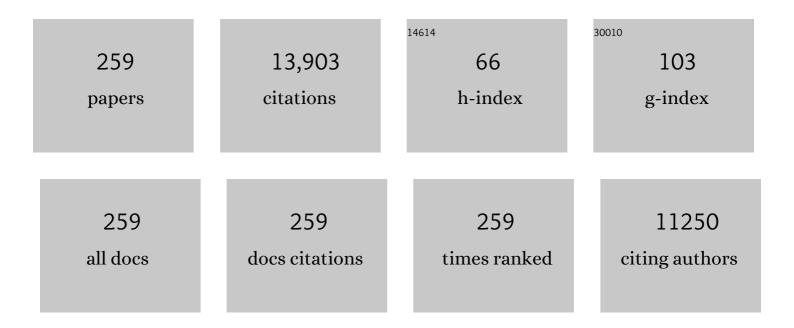
Zhao-Yin Wen

List of Publications by Year in descending order

Source: https://exaly.com/author-pdf/7994116/publications.pdf Version: 2024-02-01



ΖΗΛΟ-ΥΙΝΙ Μ/ΕΝ

#	Article	IF	CITATIONS
1	Improved cycling performances of lithium sulfur batteries with LiNO3-modified electrolyte. Journal of Power Sources, 2011, 196, 9839-9843.	4.0	457
2	A lithium anode protection guided highly-stable lithium–sulfur battery. Chemical Communications, 2014, 50, 14209-14212.	2.2	350
3	A free-standing-type design for cathodes of rechargeable Li–O2 batteries. Energy and Environmental Science, 2011, 4, 4727.	15.6	286
4	Constructing Highly Oriented Configuration by Few-Layer MoS ₂ : Toward High-Performance Lithium-Ion Batteries and Hydrogen Evolution Reactions. ACS Nano, 2015, 9, 12464-12472.	7.3	259
5	Electrochemical behaviors of a Li3N modified Li metal electrode in secondary lithium batteries. Journal of Power Sources, 2011, 196, 8091-8097.	4.0	255
6	Vinylene carbonate–LiNO3: A hybrid additive in carbonic ester electrolytes for SEI modification on Li metal anode. Electrochemistry Communications, 2015, 51, 59-63.	2.3	241
7	A nano-structured and highly ordered polypyrrole-sulfur cathode for lithium–sulfur batteries. Journal of Power Sources, 2011, 196, 6951-6955.	4.0	240
8	Highly dispersed sulfur in ordered mesoporous carbon sphere as a composite cathode for rechargeable polymer Li/S battery. Journal of Power Sources, 2011, 196, 3655-3658.	4.0	240
9	Preparation and electrochemical performance of Ag doped Li4Ti5O12. Electrochemistry Communications, 2004, 6, 1093-1097.	2.3	234
10	Lithium Ion-Conducting Glass?Ceramics of Li1.5Al0.5Ge1.5(PO4)3?xLi2O (x=0.0?0.20) with Good Electrical and Electrochemical Properties. Journal of the American Ceramic Society, 2007, 90, 2802-2806.	1.9	223
11	Main Challenges for High Performance NAS Battery: Materials and Interfaces. Advanced Functional Materials, 2013, 23, 1005-1018.	7.8	206
12	In Situ Generated Fireproof Gel Polymer Electrolyte with Li _{6.4} Ga _{0.2} La ₃ Zr ₂ O ₁₂ As Initiator and Ion onductive Filler. Advanced Energy Materials, 2019, 9, 1900611.	10.2	185
13	A shuttle effect free lithium sulfur battery based on a hybrid electrolyte. Physical Chemistry Chemical Physics, 2014, 16, 21225-21229.	1.3	171
14	Research on sodium sulfur battery for energy storage. Solid State Ionics, 2008, 179, 1697-1701.	1.3	164
15	Enhanced performance of lithium sulfur battery with self-assembly polypyrrole nanotube film as the functional interlayer. Journal of Power Sources, 2015, 273, 511-516.	4.0	159
16	An <i>in situ</i> element permeation constructed high endurance Li–LLZO interface at high current densities. Journal of Materials Chemistry A, 2018, 6, 18853-18858.	5.2	157
17	A potassium-rich iron hexacyanoferrate/dipotassium terephthalate@carbon nanotube composite used for K-ion full-cells with an optimized electrolyte. Journal of Materials Chemistry A, 2017, 5, 19017-19024.	5.2	146
18	Enhanced performance of lithium sulfur battery with polypyrrole warped mesoporous carbon/sulfur composite. Journal of Power Sources, 2014, 254, 353-359.	4.0	140

#	Article	IF	CITATIONS
19	Unraveling the Catalytic Mechanism of Co ₃ O ₄ for the Oxygen Evolution Reaction in a Li–O ₂ Battery. ACS Catalysis, 2015, 5, 73-81.	5.5	140
20	Acid induced conversion towards a robust and lithiophilic interface for Li–Li ₇ La ₃ Zr ₂ O ₁₂ solid-state batteries. Journal of Materials Chemistry A, 2019, 7, 14565-14574.	5.2	138
21	A composite of sulfur and polypyrrole–multi walled carbon combinatorial nanotube as cathode for Li/S battery. Journal of Power Sources, 2012, 206, 409-413.	4.0	135
22	Enhanced cycle performance of Li–S battery with a polypyrrole functional interlayer. Journal of Power Sources, 2014, 267, 542-546.	4.0	133
23	Composite Solid Polymer Electrolyte with Garnet Nanosheets in Poly(ethylene oxide). ACS Sustainable Chemistry and Engineering, 2019, 7, 7163-7170.	3.2	131
24	Enhanced cycle performance of a Li–S battery based on a protected lithium anode. Journal of Materials Chemistry A, 2014, 2, 19355-19359.	5.2	126
25	Sulfonic Groups Originated Dual-Functional Interlayer for High Performance Lithium–Sulfur Battery. ACS Applied Materials & Interfaces, 2017, 9, 14878-14888.	4.0	126
26	Improved electrochemical property of Ni-rich LiNi0.6Co0.2Mn0.2O2 cathode via in-situ ZrO2 coating for high energy density lithium ion batteries. Chemical Engineering Journal, 2020, 389, 124403.	6.6	125
27	Highly Adhesive Li-BN Nanosheet Composite Anode with Excellent Interfacial Compatibility for Solid-State Li Metal Batteries. ACS Nano, 2019, 13, 14549-14556.	7.3	123
28	Highly stable garnet solid electrolyte based Li-S battery with modified anodic and cathodic interfaces. Energy Storage Materials, 2018, 15, 282-290.	9.5	121
29	High-Strength Internal Cross-Linking Bacterial Cellulose-Network-Based Gel Polymer Electrolyte for Dendrite-Suppressing and High-Rate Lithium Batteries. ACS Applied Materials & Interfaces, 2018, 10, 17809-17819.	4.0	121
30	ZnO nanoarray-modified nickel foam as a lithiophilic skeleton to regulate lithium deposition for lithium-metal batteries. Journal of Materials Chemistry A, 2019, 7, 7752-7759.	5.2	120
31	A tubular polypyrrole based air electrode with improved O2 diffusivity for Li–O2 batteries. Energy and Environmental Science, 2012, 5, 7893.	15.6	119
32	Pre-modified Li3PS4 based interphase for lithium anode towards high-performance Li-S battery. Energy Storage Materials, 2018, 11, 16-23.	9.5	119
33	Flexible self-supporting graphene–sulfur paper for lithium sulfur batteries. RSC Advances, 2013, 3, 2558.	1.7	115
34	Hollow polyaniline sphere@sulfur composites for prolonged cycling stability of lithium–sulfur batteries. Journal of Materials Chemistry A, 2014, 2, 10350-10354.	5.2	114
35	Manipulating Li2O atmosphere for sintering dense Li7La3Zr2O12 solid electrolyte. Energy Storage Materials, 2019, 22, 207-217.	9.5	114
36	A gel-ceramic multi-layer electrolyte for long-life lithium sulfur batteries. Chemical Communications, 2016, 52, 1637-1640.	2.2	113

#	Article	IF	CITATIONS
37	A Li-Garnet composite ceramic electrolyte and its solid-state Li-S battery. Journal of Power Sources, 2018, 382, 190-197.	4.0	111
38	Highly disordered hard carbon derived from skimmed cotton as a high-performance anode material for potassium-ion batteries. Journal of Power Sources, 2018, 396, 533-541.	4.0	109
39	Reversible ion exchange and structural stability of garnet-type Nb-doped Li7La3Zr2O12 in water for applications in lithium batteries. Journal of Power Sources, 2015, 282, 286-293.	4.0	104
40	Enhanced performance of lithium sulfur batteries with conductive polymer modified separators. Journal of Materials Chemistry A, 2016, 4, 16968-16974.	5.2	103
41	Li/Li ₇ La ₃ Zr ₂ O ₁₂ /LiFePO ₄ All-Solid-State Battery with Ultrathin Nanoscale Solid Electrolyte. Journal of Physical Chemistry C, 2017, 121, 1431-1435.	1.5	98
42	One‣tep Solvothermal Synthesis of Nanostructured Manganese Fluoride as an Anode for Rechargeable Lithiumâ€lon Batteries and Insights into the Conversion Mechanism. Advanced Energy Materials, 2015, 5, 1401716.	10.2	97
43	Surface Acidity as Descriptor of Catalytic Activity for Oxygen Evolution Reaction in Li-O ₂ Battery. Journal of the American Chemical Society, 2015, 137, 13572-13579.	6.6	92
44	Self-catalyzed decomposition of discharge products on the oxygen vacancy sites of MoO3 nanosheets for low-overpotential Li-O2 batteries. Nano Energy, 2017, 36, 186-196.	8.2	92
45	Nanoporous Adsorption Effect on Alteration of the Li ⁺ Diffusion Pathway by a Highly Ordered Porous Electrolyte Additive for High-Rate All-Solid-State Lithium Metal Batteries. ACS Applied Materials & Interfaces, 2018, 10, 23874-23882.	4.0	90
46	In Situ Conversion of Cu ₃ P Nanowires to Mixed Ion/Electronâ€Conducting Skeleton for Homogeneous Lithium Deposition. Advanced Energy Materials, 2020, 10, 1902989.	10.2	88
47	Sustained Releaseâ€Driven Formation of Ultrastable SEI between Li ₆ PS ₅ Cl and Lithium Anode for Sulfideâ€Based Solidâ€State Batteries. Advanced Energy Materials, 2021, 11, 2002545.	10.2	87
48	Realization of the Li ⁺ domain diffusion effect <i>via</i> constructing molecular brushes on the LLZTO surface and its application in all-solid-state lithium batteries. Journal of Materials Chemistry A, 2019, 7, 27304-27312.	5.2	86
49	Two-step sintering strategy to prepare dense Li-Garnet electrolyte ceramics with high Li+ conductivity. Ceramics International, 2018, 44, 5660-5667.	2.3	82
50	Metal-organic-framework-derived N-C-Co film as a shuttle-suppressing interlayer for lithium sulfur battery. Chemical Engineering Journal, 2018, 334, 2356-2362.	6.6	82
51	Overcoming the abnormal grain growth in Ga-doped Li7La3Zr2O12 to enhance the electrochemical stability against Li metal. Ceramics International, 2019, 45, 14991-14996.	2.3	82
52	A 3D Crossâ€Linking Lithiophilic and Electronically Insulating Interfacial Engineering for Garnetâ€Type Solidâ€State Lithium Batteries. Advanced Functional Materials, 2021, 31, 2007815.	7.8	82
53	Gel polymer electrolyte with ionic liquid for high performance lithium sulfur battery. Solid State Ionics, 2012, 225, 604-607.	1.3	81
54	Synthesis of ordered mesoporous CuCo2O4 with different textures as anode material for lithium ion battery. Microporous and Mesoporous Materials, 2013, 169, 242-247.	2.2	80

#	Article	IF	CITATIONS
55	Electrochemical performance and stability of cobalt-free Ln1.2Sr0.8NiO4 (Ln=La and Pr) air electrodes for proton-conducting reversible solid oxide cells. Electrochimica Acta, 2018, 267, 269-277.	2.6	80
56	Hierarchically ordered mesoporous Co3O4 materials for high performance Li-ion batteries. Scientific Reports, 2016, 6, 19564.	1.6	79
57	The doping effect on the catalytic activity of graphene for oxygen evolution reaction in a lithium–air battery: a first-principles study. Physical Chemistry Chemical Physics, 2015, 17, 14605-14612.	1.3	77
58	From Nature to Energy Storage: A Novel Sustainable 3D Cross-Linked Chitosan–PEGGE-Based Gel Polymer Electrolyte with Excellent Lithium-Ion Transport Properties for Lithium Batteries. ACS Applied Materials & Interfaces, 2018, 10, 38526-38537.	4.0	77
59	Graphene nanosheets loaded with Pt nanoparticles with enhanced electrochemical performance for sodium–oxygen batteries. Journal of Materials Chemistry A, 2015, 3, 2568-2571.	5.2	76
60	Fe ₇ S ₈ Nanoparticles Anchored on Nitrogen-Doped Graphene Nanosheets as Anode Materials for High-Performance Sodium-Ion Batteries. ACS Applied Materials & Interfaces, 2018, 10, 29476-29485.	4.0	75
61	Preparation of dense Ta-LLZO/MgO composite Li-ion solid electrolyte: Sintering, microstructure, performance and the role of MgO. Journal of Energy Chemistry, 2019, 39, 8-16.	7.1	74
62	Air Electrode for the Lithium–Air Batteries: Materials and Structure Designs. ChemPlusChem, 2015, 80, 270-287.	1.3	73
63	Electronic and ionic co-conductive coating on the separator towards high-performance lithium–sulfur batteries. Journal of Power Sources, 2016, 306, 347-353.	4.0	72
64	A rGO–CNT aerogel covalently bonded with a nitrogen-rich polymer as a polysulfide adsorptive cathode for high sulfur loading lithium sulfur batteries. Journal of Materials Chemistry A, 2017, 5, 14775-14782.	5.2	71
65	A high-energy quinone-based all-solid-state sodium metal battery. Nano Energy, 2019, 62, 718-724.	8.2	71
66	Self-template construction of mesoporous silicon submicrocube anode for advanced lithium ion batteries. Energy Storage Materials, 2018, 15, 139-147.	9.5	70
67	In Situ Lithiophilic Layer from H ⁺ /Li ⁺ Exchange on Garnet Surface for the Stable Lithium-Solid Electrolyte Interface. ACS Applied Materials & Interfaces, 2019, 11, 35030-35038.	4.0	70
68	Local Lattice Distortion Activate Metastable Metal Sulfide as Catalyst with Stable Full Discharge–Charge Capability for Li–O ₂ Batteries. Nano Letters, 2017, 17, 3518-3526.	4.5	68
69	Mesoporous carbon nitride loaded with Pt nanoparticles as a bifunctional air electrode for rechargeable lithium-air battery. Journal of Solid State Electrochemistry, 2012, 16, 1863-1868.	1.2	67
70	<i>In situ</i> formation of LiF decoration on a Li-rich material for long-cycle life and superb low-temperature performance. Journal of Materials Chemistry A, 2019, 7, 11513-11519.	5.2	67
71	Grain boundary modification in garnet electrolyte to suppress lithium dendrite growth. Chemical Engineering Journal, 2021, 411, 128508.	6.6	66
72	In situ fabricated ceramic/polymer hybrid electrolyte with vertically aligned structure for solid-state lithium batteries. Energy Storage Materials, 2021, 36, 171-178.	9.5	62

#	Article	IF	CITATIONS
73	Enhanced electrochemical performance promoted by monolayer graphene and void space in silicon composite anode materials. Nano Energy, 2016, 27, 647-657.	8.2	61
74	Recent advances in anodic interface engineering for solid-state lithium-metal batteries. Materials Horizons, 2020, 7, 1667-1696.	6.4	60
75	Suppressing the dissolution of polysulfides with cosolvent fluorinated diether towards high-performance lithium sulfur batteries. Physical Chemistry Chemical Physics, 2016, 18, 29293-29299.	1.3	59
76	Research activities in Shanghai Institute of Ceramics, Chinese Academy of Sciences on the solid electrolytes for sodium sulfur batteries. Journal of Power Sources, 2008, 184, 641-645.	4.0	58
77	Method Using Water-Based Solvent to Prepare Li ₇ La ₃ Zr ₂ O ₁₂ Solid Electrolytes. ACS Applied Materials & Interfaces, 2018, 10, 17147-17155.	4.0	58
78	Improving the electrochemical performance of Li-rich Li1.2Ni0.2Mn0.6O2 by using Ni-Mn oxide surface modification. Journal of Power Sources, 2018, 390, 13-19.	4.0	57
79	Robust and Conductive Red MoSe ₂ for Stable and Fast Lithium Storage. ACS Nano, 2018, 12, 4010-4018.	7.3	57
80	On the dispersion of lithium-sulfur battery cathode materials effected by electrostatic and stereo-chemical factors of binders. Journal of Power Sources, 2016, 324, 455-461.	4.0	56
81	Interconnected CoFe ₂ O ₄ –Polypyrrole Nanotubes as Anode Materials for High Performance Sodium Ion Batteries. ACS Applied Materials & Interfaces, 2017, 9, 36927-36935.	4.0	56
82	Recent Progress in Liquid Electrolyte-Based Li–S Batteries: Shuttle Problem and Solutions. Electrochemical Energy Reviews, 2018, 1, 599-624.	13.1	56
83	Anchoring succinonitrile by solvent-Li+ associations for high-performance solid-state lithium battery. Chemical Engineering Journal, 2021, 406, 126754.	6.6	56
84	Carbon-coated isotropic natural graphite spheres as anode material for lithium-ion batteries. Ceramics International, 2017, 43, 9458-9464.	2.3	53
85	Mesoporous Co3O4 with different porosities as catalysts for the lithium–oxygen cell. Solid State Ionics, 2012, 225, 598-603.	1.3	52
86	Molybdenum-doped lithium-rich layered-structured cathode material Li1.2Ni0.2Mn0.6O2 with high specific capacity and improved rate performance. Electrochimica Acta, 2015, 168, 234-239.	2.6	52
87	A hybrid electrolyte for long-life semi-solid-state lithium sulfur batteries. Journal of Materials Chemistry A, 2017, 5, 13971-13975.	5.2	52
88	Enhancing metallic lithium battery performance by tuning the electrolyte solution structure. Journal of Materials Chemistry A, 2018, 6, 1612-1620.	5.2	52
89	Lattice Incorporation of Cu ²⁺ into the BaCe _{0.7} Zr _{0.1} Y _{0.1} Yb _{0.1} O _{3â^{-^}î} Electrolyte on Boosting Its Sintering and Proton-Conducting Abilities for Reversible Solid Oxide Cells. ACS Applied Materials & amp: Interfaces. 2018. 10. 42387-42396.	4.0	52
90	Porous carbon-coated NaTi ₂ (PO ₄) ₃ with superior rate and low-temperature properties. Journal of Materials Chemistry A, 2018, 6, 2365-2370.	5.2	51

#	Article	IF	CITATIONS
91	A novel strategy to prepare Ge@C/rGO hybrids as high-rate anode materials for lithium ion batteries. Journal of Power Sources, 2017, 342, 521-528.	4.0	50
92	Self-supported mesoporous FeCo2O4 nanosheets as high capacity anode material for sodium-ion battery. Chemical Engineering Journal, 2017, 330, 764-773.	6.6	50
93	Cobalt Phosphide Nanoflake-Induced Flower-like Sulfur for High Redox Kinetics and Fast Ion Transfer in Lithium-Sulfur Batteries. ACS Applied Materials & Interfaces, 2020, 12, 49626-49635.	4.0	50
94	Leakage behavior of toxic substances of naphthalene sulfonate-formaldehyde condensation from cement based materials. Journal of Environmental Management, 2020, 255, 109934.	3.8	49
95	Sol–gel synthesis of Mg2+ stabilized Na-β″/β-Al2O3 solid electrolyte for sodium anode battery. Journal of Alloys and Compounds, 2014, 613, 80-86.	2.8	48
96	Sintering, micro-structure and Li+ conductivity of Li7â^'La3Zr2â^'Nb O12/MgO (x = 0.2–0.7) Li-Garnet composite ceramics. Ceramics International, 2019, 45, 56-63.	2.3	48
97	Enhancement of long stability of Li–S battery by thin wall hollow spherical structured polypyrrole based sulfur cathode. RSC Advances, 2014, 4, 21612-21618.	1.7	47
98	Facile synthesis of the sandwich-structured germanium/reduced graphene oxide hybrid: an advanced anode material for high-performance lithium ion batteries. Journal of Materials Chemistry A, 2017, 5, 13430-13438.	5.2	47
99	An ion-conductive Li1.5Al0.5Ge1.5(PO4)3-based composite protective layer for lithium metal anode in lithium-sulfur batteries. Journal of Power Sources, 2018, 377, 36-43.	4.0	47
100	Effects of alumina whisker in (PEO)8–LiClO4-based composite polymer electrolytes. Solid State Ionics, 2002, 148, 185-191.	1.3	46
101	Influence of La2Zr2O7 Additive on Densification and Li+ Conductivity for Ta-Doped Li7La3Zr2O12 Garnet. Jom, 2016, 68, 2593-2600.	0.9	46
102	Synthesis of α-MnO ₂ nanowires modified by Co ₃ O ₄ nanoparticles as a high-performance catalyst for rechargeable Li–O ₂ batteries. Physical Chemistry Chemical Physics, 2016, 18, 926-931.	1.3	46
103	In-situ constructed lithium-salt lithiophilic layer inducing bi-functional interphase for stable LLZO/Li interface. Energy Storage Materials, 2022, 47, 61-69.	9.5	46
104	Carbon Disulfide Cosolvent Electrolytes for High-Performance Lithium Sulfur Batteries. ACS Applied Materials & Interfaces, 2016, 8, 34379-34386.	4.0	45
105	Synthesis and characterization of perovskite-type (Li,Sr)(Zr,Nb)O3 quaternary solid electrolyte for all-solid-state batteries. Journal of Power Sources, 2016, 306, 623-629.	4.0	45
106	Scalable synthesis of hierarchical porous Ge/rGO microspheres with an ultra-long cycling life for lithium storage. Journal of Power Sources, 2018, 396, 124-133.	4.0	45
107	Mixed-carbon-coated LiMn0.4Fe0.6PO4 nanopowders with excellent high rate and low temperature performances for lithium-ion batteries. Electrochimica Acta, 2016, 196, 377-385.	2.6	44
108	The long life-span of a Li-metal anode enabled by a protective layer based on the pyrolyzed N-doped binder network. Journal of Materials Chemistry A, 2017, 5, 9339-9349.	5.2	44

#	Article	IF	CITATIONS
109	Microstructure boosting the cycling stability of LiNi0.6Co0.2Mn0.2O2 cathode through Zr-based dual modification. Energy Storage Materials, 2021, 36, 179-185.	9.5	44
110	Research on spray-dried lithium titanate as electrode materials for lithium ion batteries. Journal of Power Sources, 2005, 146, 670-673.	4.0	43
111	Cobalt-substituted Na0.44Mn1-xCoxO2: phase evolution and a high capacity positive electrode for sodium-ion batteries. Electrochimica Acta, 2016, 213, 496-503.	2.6	43
112	From nanomelting to nanobeads: nanostructured Sb _x Bi _{1â^'x} alloys anchored in three-dimensional carbon frameworks as a high-performance anode for potassium-ion batteries. Journal of Materials Chemistry A, 2019, 7, 27041-27047.	5.2	43
113	Hierarchical mesoporous iron-based fluoride with partially hollow structure: facile preparation and high performance as cathode material for rechargeable lithium ion batteries. Physical Chemistry Chemical Physics, 2014, 16, 8556.	1.3	42
114	A conductive selenized polyacrylonitrile cathode material for re-chargeable lithium batteries with long cycle life. Journal of Materials Chemistry A, 2015, 3, 19815-19821.	5.2	42
115	Towards improved structural stability and electrochemical properties of a Li-rich material by a strategy of double gradient surface modification. Nano Energy, 2019, 61, 411-419.	8.2	42
116	Trimethylsilyl Chloride-Modified Li Anode for Enhanced Performance of Li–S Cells. ACS Applied Materials & Interfaces, 2016, 8, 16386-16395.	4.0	41
117	One-step microwave synthesized core–shell structured selenium@carbon spheres as cathode materials for rechargeable lithium batteries. Chemical Communications, 2016, 52, 5613-5616.	2.2	41
118	Constructing dual interfacial modification by synergetic electronic and ionic conductors: Toward high-performance LAGP-Based Li-S batteries. Energy Storage Materials, 2019, 23, 299-305.	9.5	40
119	Synthesis and properties of poly(1,3-dioxolane) <i>in situ</i> quasi-solid-state electrolytes <i>via</i> a rare-earth triflate catalyst. Chemical Communications, 2021, 57, 7934-7937.	2.2	39
120	Improving the electrochemical properties of high-energy cathode material LiNi0.5Co0.2Mn0.3O2 by Zr doping and sintering in oxygen. Solid State Ionics, 2015, 279, 11-17.	1.3	38
121	Cobalt-Metal-Based Cathode for Lithium–Oxygen Battery with Improved Electrochemical Performance. ACS Catalysis, 2016, 6, 4149-4153.	5.5	38
122	Wave-like free-standing NiCo2O4 cathode for lithium–oxygen battery with high discharge capacity. Journal of Power Sources, 2015, 294, 593-601.	4.0	37
123	Solid polymer electrolyte based on thermoplastic polyurethane and its application in all-solid-state lithium ion batteries. Solid State Ionics, 2017, 309, 15-21.	1.3	37
124	Atomic-Thick TiO ₂ (B) Nanosheets Decorated with Ultrafine Co ₃ O ₄ Nanocrystals As a Highly Efficient Catalyst for Lithium–Oxygen Battery. ACS Applied Materials & Interfaces, 2018, 10, 41398-41406.	4.0	37
125	Open mesoporous spherical shell structured Co3O4with highly efficient catalytic performance in Li–O2batteries. Journal of Materials Chemistry A, 2015, 3, 7600-7606.	5.2	36
126	The enhanced performance of Li–S battery with P14YRTFSI-modified electrolyte. Solid State Ionics, 2014, 262, 174-178.	1.3	35

#	Article	IF	CITATIONS
127	Favorable lithium deposition behaviors on flexible carbon microtube skeleton enable a high-performance lithium metal anode. Journal of Materials Chemistry A, 2018, 6, 19159-19166.	5.2	35
128	Disordered carbon tubes based on cotton cloth for modulating interface impedance in β′′-Al ₂ O ₃ -based solid-state sodium metal batteries. Journal of Materials Chemistry A, 2018, 6, 12623-12629.	5.2	35
129	In situ synthesis of core-shell structured Ge@NC hybrids as high performance anode material for lithium-ion batteries. Chemical Engineering Journal, 2019, 360, 1301-1309.	6.6	35
130	Ultrathin TiO2 surface layer coated TiN nanoparticles in freestanding film for high sulfur loading Li-S battery. Chemical Engineering Journal, 2020, 399, 125674.	6.6	35
131	High-performance phosphorus-modified SiO/C anode material for lithium ion batteries. Ceramics International, 2018, 44, 18509-18515.	2.3	34
132	A lithium-MXene composite anode with high specific capacity and low interfacial resistance for solid-state batteries. Energy Storage Materials, 2022, 45, 934-940.	9.5	34
133	Performance and stability of BaCe0.8â^'xZr0.2InxO3â^'Î^based materials and reversible solid oxide cells working at intermediate temperature. International Journal of Hydrogen Energy, 2017, 42, 28549-28558.	3.8	33
134	Synthesis of Ga-doped Li7La3Zr2O12 solid electrolyte with high Li+ ion conductivity. Ceramics International, 2021, 47, 2123-2130.	2.3	33
135	Robust Conversion-Type Li/Garnet interphases from metal salt solutions. Chemical Engineering Journal, 2021, 417, 129158.	6.6	33
136	Enhanced cycle performance of a Na/NiCl 2 battery based on Ni particles encapsulated with Ni 3 S 2 layer. Journal of Power Sources, 2017, 340, 411-418.	4.0	32
137	Tailoring a micro-nanostructured electrolyte-oxygen electrode interface for proton-conducting reversible solid oxide cells. Journal of Power Sources, 2020, 449, 227498.	4.0	32
138	Preparation of Nanocomposite Polymer Electrolyte via In Situ Synthesis of SiO2 Nanoparticles in PEO. Nanomaterials, 2020, 10, 157.	1.9	32
139	Influence of a surface modified Li anode on the electrochemical performance of Li–S batteries. RSC Advances, 2016, 6, 40270-40276.	1.7	31
140	Anchoring Nanostructured Manganese Fluoride on Few-Layer Graphene Nanosheets as Anode for Enhanced Lithium Storage. ACS Applied Materials & Interfaces, 2016, 8, 1819-1826.	4.0	31
141	Effects of porous support microstructure enabled by the carbon microsphere pore former on the performance of proton-conducting reversible solid oxide cells. International Journal of Hydrogen Energy, 2018, 43, 20050-20058.	3.8	30
142	Composite Hybrid Quasi-Solid Electrolyte for High-Energy Lithium Metal Batteries. ACS Applied Energy Materials, 2021, 4, 7973-7982.	2.5	30
143	Construction of hierarchical NiS@C/rGO heterostructures for enhanced sodium storage. Chemical Engineering Journal, 2022, 435, 134633.	6.6	30
144	A new gridding cyanoferrate anode material for lithium and sodium ion batteries: Ti0.75Fe0.25[Fe(CN)6]0.96·1.9H2O with excellent electrochemical properties. Journal of Power Sources, 2016, 314, 35-38.	4.0	29

#	Article	IF	CITATIONS
145	Preparation and electrochemical properties of Li[Ni1/3Co1/3Mn1â^'x/3Zrx/3]O2 cathode materials for Li-ion batteries. Journal of Power Sources, 2007, 174, 544-547.	4.0	28
146	Low-cost shape-control synthesis of porous carbon film on β″-alumina ceramics for Na-based battery application. Journal of Power Sources, 2012, 219, 1-8.	4.0	28
147	Suppressing Redox Shuttle with MXene-Modified Separators for Li–O ₂ Batteries. ACS Applied Materials & Interfaces, 2021, 13, 30766-30775.	4.0	28
148	Nickel nanowire network coating to alleviate interfacial polarization for Na-beta battery applications. Journal of Power Sources, 2013, 240, 786-795.	4.0	27
149	None-Mother-Powder Method to Prepare Dense Li-Garnet Solid Electrolytes with High Critical Current Density. ACS Applied Energy Materials, 0, , .	2.5	27
150	A novel Bi-doped borosilicate glass as sealant for sodium sulfur battery. Part 1: Thermophysical characteristics and structure. Journal of Power Sources, 2010, 195, 384-388.	4.0	26
151	Controlling uniform deposition of discharge products at the nanoscale for rechargeable Na–O ₂ batteries. Journal of Materials Chemistry A, 2016, 4, 7238-7244.	5.2	26
152	Assembly of Multifunctional Ni ₂ P/NiS _{0.66} Heterostructures and Their Superstructure for High Lithium and Sodium Anodic Performance. ACS Applied Materials & Interfaces, 2017, 9, 28549-28557.	4.0	26
153	A facile method for the synthesis of a sintering dense nano-grained Na ₃ Zr ₂ Si ₂ PO ₁₂ Na ⁺ -ion solid-state electrolyte. Chemical Communications, 2021, 57, 4023-4026.	2.2	26
154	Preparation and characterization of carbon-coated Li[Ni1/3Co1/3Mn1/3]O2 cathode material for lithium-ion batteries. Journal of Solid State Electrochemistry, 2010, 14, 1807-1811.	1.2	24
155	Analysis of Structure and Electrochemistry of Selenium-Containing Conductive Polymer Materials for Rechargeable Lithium Batteries. Journal of the Electrochemical Society, 2016, 163, A654-A659.	1.3	24
156	A High-Rate Ionic Liquid Lithium-O ₂ Battery with LiOH Product. Journal of Physical Chemistry C, 2017, 121, 5968-5973.	1.5	24
157	Nâ€Doped Graphene Decorated with Fe/Fe ₃ N/Fe ₄ N Nanoparticles as a Highly Efficient Cathode Catalyst for Rechargeable Liâ^'O ₂ Batteries. ChemElectroChem, 2018, 5, 2435-2441.	1.7	24
158	High rate LiMn2O4/carbon nanotube composite prepared by a two-step hydrothermal process. Journal of Power Sources, 2014, 268, 491-497.	4.0	23
159	Enhancing the electrochemical performances of LiNi0.5Mn1.5O4 by Co3O4 surface coating. Journal of Alloys and Compounds, 2018, 762, 163-170.	2.8	23
160	Highly active mixed-valent MnO _x spheres constructed by nanocrystals as efficient catalysts for long-cycle Li–O ₂ batteries. Journal of Materials Chemistry A, 2016, 4, 17129-17137.	5.2	22
161	New glass-ceramic sealants for Na/S battery. Journal of Solid State Electrochemistry, 2010, 14, 1735-1740.	1.2	21
162	A selenium@polypyrrole hollow sphere cathode for rechargeable lithium batteries. RSC Advances, 2015, 5, 20346-20350.	1.7	21

#	Article	IF	CITATIONS
163	FeS2 microsphere as cathode material for rechargeable lithium batteries. Solid State Ionics, 2016, 290, 47-52.	1.3	21
164	Microregion Welding Strategy Prevents the Formation of Inactive Sulfur Species for Highâ€Performance Li–S Battery. Advanced Energy Materials, 2021, 11, 2102024.	10.2	21
165	Searching for low-cost Li MO compounds for compensating Li-loss in sintering of Li-Garnet solid electrolyte. Journal of Materiomics, 2019, 5, 221-228.	2.8	20
166	Gallium-substituted Nasicon Na3Zr2Si2PO12 solid electrolytes. Journal of Alloys and Compounds, 2021, 855, 157501.	2.8	20
167	Achieving high critical current density in Ta-doped Li7La3Zr2O12/MgO composite electrolytes. Journal of Alloys and Compounds, 2021, 856, 157222.	2.8	20
168	Hollow-Sphere-Structured Na ₄ Fe ₃ (PO ₄) ₂ (P ₂ O ₇)/C as a Cathode Material for Sodium-Ion Batteries. ACS Applied Materials & Interfaces, 2021, 13, 25972-25980.	4.0	20
169	Realizing the growth of nano-network Li2O2 film on defect-rich holey Co9S8 nanosheets for Li-O2 battery. Chemical Engineering Journal, 2020, 396, 125228.	6.6	20
170	Mechanochemical synthesis of Na-β/β″-Al2O3. Journal of Solid State Electrochemistry, 2010, 14, 1821-1827.	1.2	19
171	Improved performance of Li-S battery with hybrid electrolyte by interface modification. Solid State lonics, 2017, 300, 67-72.	1.3	19
172	Enhanced stability performance of nickel nanowire with 3D conducting network for planar sodium-nickel chloride batteries. Journal of Power Sources, 2017, 360, 345-352.	4.0	19
173	Improvement of density and electrochemical performance of garnet-type Li7La3Zr2O12 for solid-state lithium metal batteries enabled by W and Ta co-doping strategy. Materials Today Energy, 2022, 27, 101034.	2.5	19
174	Facile synthesis of Fe@Fe2O3 core-shell nanowires as O2 electrode for high-energy Li-O2 batteries. Journal of Solid State Electrochemistry, 2016, 20, 1831-1836.	1.2	18
175	A novel thin solid electrolyte film and its application in all-solid-state battery at room temperature. Ionics, 2018, 24, 1545-1551.	1.2	18
176	Multi-substituted garnet-type electrolytes for solid-state lithium batteries. Ceramics International, 2020, 46, 5489-5494.	2.3	18
177	Ni-less cathode with 3D free-standing conductive network for planar Na-NiCl2 batteries. Chemical Engineering Journal, 2020, 387, 124059.	6.6	18
178	Fabrication of dense CaZr0.90In0.10O3â^`î´ ceramics from the fine powders prepared by an optimized solid-state reaction method. Solid State Ionics, 2008, 179, 1108-1111.	1.3	17
179	Worm-like mesoporous structured iron-based fluoride: Facile preparation and application as cathodes for rechargeable lithium ion batteries. Journal of Power Sources, 2013, 244, 306-311.	4.0	17
180	Self-Repairing Function of Ni ₃ S ₂ Layer on Ni Particles in the Na/NiCl ₂ Cells with the Addition of Sulfur in the Catholyte. ACS Applied Materials & Interfaces, 2017, 9, 21234-21242.	4.0	17

#	Article	IF	CITATIONS
181	La ₄ NiLiO ₈ -Shielded Layered Cathode Materials for Emerging High-Performance Safe Batteries. ACS Applied Materials & Interfaces, 2020, 12, 826-835.	4.0	17
182	High-Rate and Long-Life Intermediate-Temperature Na–NiCl ₂ Battery with Dual-Functional Ni–Carbon Composite Nanofiber Network. ACS Applied Materials & Interfaces, 2020, 12, 24767-24776.	4.0	17
183	Introducing a conductive pillar: a polyaniline intercalated layered titanate for high-rate and ultra-stable sodium and potassium ion storage. Chemical Communications, 2020, 56, 8392-8395.	2.2	17
184	Reduced free-standing Co ₃ O ₄ @Ni cathode for lithium–oxygen batteries with enhanced electrochemical performance. RSC Advances, 2016, 6, 16263-16267.	1.7	16
185	Organic Polysulfides Based on â^'Sâ^'Sâ^'Sâ^' Structure as Additives or Cosolvents for High Performance Lithium‣ulfur Batteries. ChemElectroChem, 2018, 5, 1717-1723.	1.7	16
186	An investigation of poly(ethylene oxide)/saponite-based composite electrolytes. Journal of Power Sources, 2003, 119-121, 427-431.	4.0	15
187	Influence of In doping on the structure, stability and electrical conduction behavior of Ba(Ce,Ti)O3 solid solution. Journal of Alloys and Compounds, 2013, 554, 378-384.	2.8	15
188	Enhanced proton conduction of BaZr0.9Y0.1O3-δ by hybrid doping of ZnO and Na3PO4. Solid State Ionics, 2015, 281, 6-11.	1.3	15
189	In Situ Self-Developed Nanoscale MnO/MEG Composite Anode Material for Lithium-Ion Battery. Journal of the Electrochemical Society, 2016, 163, A722-A726.	1.3	15
190	High-performance lithium storage in an ultrafine manganese fluoride nanorod anode with enhanced electrochemical activation based on conversion reaction. Physical Chemistry Chemical Physics, 2016, 18, 3780-3787.	1.3	15
191	Study of CaZr0.9In0.1O3â^î^ based reversible solid oxide cells with tubular electrode supported structure. International Journal of Hydrogen Energy, 2017, 42, 23189-23197.	3.8	15
192	Conformal, nanoscale γ-Al2O3 coating of garnet conductors for solid-state lithium batteries. Solid State Ionics, 2019, 342, 115063.	1.3	15
193	A new high-capacity cathode for all-solid-state lithium sulfur battery. Solid State Ionics, 2020, 357, 115500.	1.3	15
194	Functional binder for high-performance Li–O2 batteries. Journal of Power Sources, 2013, 244, 614-619.	4.0	14
195	Porous iron oxide coating on β″-alumina ceramics for Na-based batteries. Solid State Ionics, 2014, 262, 133-137.	1.3	14
196	Studies of rare earth elements to distinguish nephrite samples from different deposits using direct current glow discharge mass spectrometry. Journal of Analytical Atomic Spectrometry, 2014, 29, 2064-2071.	1.6	14
197	Enhancing cyclability and rate performance of Li2MoO4 by carbon coating. Materials Letters, 2016, 177, 54-57.	1.3	13
198	Influence of Cu ²⁺ doping concentration on the catalytic activity of Cu _x Co _{3â^'x} O ₄ for rechargeable Li‑O ₂ batteries. Journal of Materials Chemistry A, 2017, 5, 18569-18576.	5.2	13

#	Article	IF	CITATIONS
199	Ionic activation <i>via</i> a hybrid IL–SSE interfacial layer for Li–O ₂ batteries with 99.5% coulombic efficiency. Journal of Materials Chemistry A, 2018, 6, 12945-12949.	5.2	13
200	Dual Substitution and Spark Plasma Sintering to Improve Ionic Conductivity of Garnet Li7La3Zr2O12. Nanomaterials, 2019, 9, 721.	1.9	13
201	Nanoporous ceramic-poly(ethylene oxide) composite electrolyte for sodium metal battery. Materials Letters, 2019, 236, 13-15.	1.3	13
202	Coupling solid and soluble catalysts toward stable Li anode for high-performance Li–O2 batteries. Energy Storage Materials, 2020, 28, 342-349.	9.5	13
203	Oximation reaction induced reduced graphene oxide gas sensor for formaldehyde detection. Journal of Saudi Chemical Society, 2020, 24, 364-373.	2.4	13
204	Electrochemical performance of NiCl2 with Br-free molten salt electrolyte in high power thermal batteries. Science China Technological Sciences, 2021, 64, 91-97.	2.0	13
205	Sulfonated Bacterial Cellulose-Based Functional Gel Polymer Electrolyte for Li–O ₂ Batteries with Lil as a Redox Mediator. ACS Sustainable Chemistry and Engineering, 2021, 9, 13883-13892.	3.2	13
206	A novel facile way to synthesize proton-conducting Ba(Ce,Zr,Y)O3 solid solution with improved sinterability and electrical performance. Journal of the European Ceramic Society, 2015, 35, 2109-2117.	2.8	12
207	Fabrication and characterization of a double-layer electrolyte membrane for BaCeO 3 -based reversible solid oxide cells (RSOCs). Solid State Ionics, 2017, 308, 167-172.	1.3	11
208	One Step Fabrication of <scp>Co₃O₄â€PPy</scp> Cathode for Lithiumâ€ <scp>O₂</scp> Batteries. Chinese Journal of Chemistry, 2017, 35, 35-40.	2.6	11
209	Constructing a charged-state Na-NiCl2 battery with NiCl2/graphene aerogel composite as cathode. Chemical Engineering Journal, 2021, 421, 127853.	6.6	11
210	A robust air electrode supported proton-conducting reversible solid oxide cells prepared by low temperature co-sintering. Journal of Power Sources, 2021, 492, 229602.	4.0	11
211	Modified Pechini Synthesis of Proton onducting Ba(Ce,Ti)O ₃ and Comparative Studies of the Effects of Acceptors on its Structure, Stability, Sinterability, and Conductivity. Journal of the American Ceramic Society, 2014, 97, 1103-1109.	1.9	10
212	Enhanced conductivity of lanthanum niobate proton conductor by A and B-site co-doping: Synthesis, phase, microstructure and transport properties. Solid State Ionics, 2014, 268, 326-329.	1.3	10
213	Controlled construction of 3D hierarchical manganese fluoride nanostructures via an oleylamine-assisted solvothermal route with high performance for rechargeable lithium ion batteries. RSC Advances, 2016, 6, 27170-27176.	1.7	10
214	Synthesis of graphene-modified Li3V2(PO4)3 with superior electrochemical properties via a catalytic solid-state-reaction process. Journal of Alloys and Compounds, 2017, 717, 1-7.	2.8	10
215	A hydrogel-enabled free-standing polypyrrole cathode film for potassium ion batteries with high mass loading and low-temperature stability. Journal of Materials Chemistry A, 2021, 9, 15045-15050.	5.2	10
216	A rechargeable all-solid-state sodium peroxide (Na ₂ O ₂) battery with low overpotential. Journal Physics D: Applied Physics, 2021, 54, 174005.	1.3	10

#	Article	IF	CITATIONS
217	A Janus Li1.5Al0.5Ge1.5(PO4)3 with high critical current density for high-voltage lithium batteries. Chemical Engineering Journal, 2022, 429, 132506.	6.6	10
218	Active-Site-Specific Structural Engineering Enabled Ultrahigh Rate Performance of the NaLi ₃ Fe ₃ (PO ₄) ₂ (P ₂ O ₇) Cathode for Lithium-Ion Batteries. ACS Applied Materials & Interfaces, 2022, 14, 11255-11263.	4.0	10
219	A hybrid solid electrolyte for high-energy solid-state sodium metal batteries. Applied Physics Letters, 2022, 120, .	1.5	10
220	Electrical conductivity of fully densified nano CaZr0.90In0.10O3â^î́r ceramics prepared by a water-based gel precipitation method. Solid State Ionics, 2009, 180, 154-159.	1.3	9
221	Suppressing Self-Discharge of Vanadium Diboride by Zwitterionicity of the Polydopamine Coating Layer. ACS Applied Materials & Interfaces, 2019, 11, 5123-5128.	4.0	9
222	Li 1.5 Al 0.5 Ge 1.5 (PO 4) 3 Ceramic Based Lithiumâ€Sulfur Batteries with High Cycling Stability Enabled by a Dual Confinement Effect for Polysulfides. ChemElectroChem, 2020, 7, 4093-4100.	1.7	9
223	MOF/Poly(Ethylene Oxide) Composite Polymer Electrolyte for Solid-state Lithium Battery. Wuji Cailiao Xuebao/Journal of Inorganic Materials, 2021, 36, 332.	0.6	9
224	Design of solid-state sodium-ion batteries with high mass-loading cathode by porous-dense bilayer electrolyte. Journal of Materiomics, 2021, 7, 1352-1357.	2.8	9
225	Scandia-stabilized zirconia-impregnated (La, Sr)MnO3 cathode for tubular solid oxide fuel cells. Journal of Solid State Electrochemistry, 2010, 14, 1923-1928.	1.2	8
226	Spray drying derived wrinkled pea-shaped carbon-matrixed KVP2O7 as a cathode material for potassium-ion batteries. Journal of Alloys and Compounds, 2021, 884, 161126.	2.8	8
227	Double-functional 3D cross-linking carbon fiber with Sn particle coating layer for improving interfacial performance of Na-β″-Al2O3 batteries. Chemical Engineering Journal, 2022, 433, 133545.	6.6	8
228	Proton conducting CaZr0.9In0.1O3-δ ceramic membrane prepared by tape casting. Solid State Ionics, 2012, 225, 291-296.	1.3	7
229	The Influence of Electrode Microstructure on the Performance of Free-Standing Cathode for Aprotic Lithium-Oxygen Battery. Jom, 2016, 68, 2585-2592.	0.9	7
230	Improving the rate and low-temperature performance of LiFePO4 by tailoring the form of carbon coating from amorphous to graphene-like. Journal of Solid State Electrochemistry, 2018, 22, 797-805.	1.2	7
231	Reversible AlCl4â^'/Al2Cl7â^' conversion in a hybrid Na–Al battery. Journal of Power Sources, 2020, 453, 227843.	4.0	7
232	Double-Faced Bond Coupling to Induce an Ultrastable Lithium/Li ₆ PS ₅ Cl Interface for High-Performance All-Solid-State Batteries. ACS Applied Materials & Interfaces, 2022, 14, 11950-11961.	4.0	7
233	Improvement of lithium storage performance of Sn-alloy anode materials by a polypyrrole protective layer. Journal of Power Sources, 2015, 274, 1100-1106.	4.0	6
234	CNT@MnO ₂ Hybrid as Cathode Catalysts Toward Longâ€Life Lithium Oxygen Batteries. ChemistrySelect, 2016, 1, 6749-6754.	0.7	6

#	Article	IF	CITATIONS
235	Ultrathin, Compacted Gel Polymer Electrolytes Enable Highâ€Energy and Stableâ€Cycling 4â€V Lithiumâ€Metal Batteries. ChemElectroChem, 2020, 7, 3656-3662.	1.7	5
236	Synthesis, sinterability, conductivity and reducibility of K+ and W6+ double doped La2Mo2O9. Solid State Ionics, 2015, 276, 90-97.	1.3	4
237	Protected Sulfur Cathode with Mixed Conductive Coating Layer for Lithium Sulfur Battery. Jom, 2016, 68, 2601-2606.	0.9	4
238	Introducing a cell moisturizer: organogel nano-beads with rapid response to electrolytes for Prussian white analogue based non-aqueous potassium ion battery. Chemical Communications, 2020, 56, 9719-9722.	2.2	4
239	Ultrathin, dense, hybrid polymer/ceramic gel electrolyte for high energy lithium metal batteries. Materials Letters, 2020, 279, 128480.	1.3	4
240	Understanding the influencing factors of porous cathode contributions to the impedance of a sodium-nickel chloride (ZEBRA) battery. Functional Materials Letters, 2021, 14, 2141002.	0.7	4
241	Improved protonic conductivity and Vickers hardness for lanthanum tungstate with potassium doping (La,K)28â^'W4+O54+. Solid State Ionics, 2015, 278, 69-77.	1.3	3
242	Long life anode material sodium titanate synthesized by a moderate method. Materials Letters, 2017, 186, 326-329.	1.3	3
243	Composites of Li-Al-B-Si-O glass and \hat{l}^2 -Al2O3 for LTCC-silicon heterogeneous integration applications. Ceramics International, 2018, 44, S141-S144.	2.3	3
244	Strain buffering effect of quasi-amorphous disordered microstructure enabling long-term fast sodium storage performance. Journal of Materials Chemistry A, 2019, 7, 574-585.	5.2	3
245	Multiple Nanosheets Assembled Nanoflowerâ€like MnO 2 to Anchor Polysulfides for Improving Electrochemical Performance in Lithium Sulfur Batteries. ChemistrySelect, 2019, 4, 7102-7107.	0.7	3
246	FeNi-LDH Intercalation for Suppressing the Self-Discharge of the VB2–Air Battery. ACS Applied Materials & Interfaces, 2020, 12, 8219-8224.	4.0	3
247	Submicrometer Rod-Structured Na ₇ V ₄ (P ₂ O ₇) ₄ (PO ₄)/C as a Cathode Material for Sodium-Ion Batteries. ACS Applied Energy Materials, 2021, 4, 10298-10305.	2.5	3
248	New Applications of Solid State Ionics. Wuji Cailiao Xuebao/Journal of Inorganic Materials, 2013, 28, 1163-1164.	0.6	3
249	Synthesis of Na-β″/β-Al ₂ O ₃ nanorods in an ionic liquid. Journal of Materials Research, 2013, 28, 2017-2022.	1.2	2
250	Anodic electrochemical mechanism and performance dominant factors of the VB2-air battery. Chemical Engineering Journal, 2020, 388, 124257.	6.6	2
251	<i>In situ</i> Lithiophilic ZnO Layer Constructed <i>using</i> Aqueous Strategy for a Stable Li-Garnet Interface. Wuli Huaxue Xuebao/ Acta Physico - Chimica Sinica, 2020, .	2.2	2
252	Improvement of the sealing performance of sodium anode battery by an in-situ gradient modification method. Solid State Ionics, 2013, 236, 11-15.	1.3	1

#	Article	IF	CITATIONS
253	Improvement of the sealing performance for sodium anode based battery by interface optimization of alpha-Al2O3/glass sealant. Solid State Ionics, 2014, 263, 140-145.	1.3	1
254	An in-situ alloyed Ni-Fe Co-reaction electrode for high-stability and high-rate Na-metal halide batteries. Materials Today Energy, 2022, 23, 100894.	2.5	1
255	In Situ Partial Pyrolysis of Sodium Carboxymethyl Cellulose Constructing Hierarchical Pores in the Silicon Anode for Lithium-Ion Batteries. ACS Applied Energy Materials, 2022, 5, 380-386.	2.5	1
256	VN and SeS ₂ embedded porous carbon-nanofiber film as a free-standing electrode for improved Li–SeS ₂ batteries. Chemical Communications, 0, , .	2.2	1
257	A Stable and Easily Sintering SrCeO3-Based Proton Conductor by a Polymerizable Complex Method. Integrated Ferroelectrics, 2010, 115, 25-33.	0.3	0
258	Synthesis and characterization of CaZr0.95In0.05O3â^îΖBaCe0.9Y0.1O3â^Î, composite ceramics. Solid State Ionics, 2015, 275, 39-42.	1.3	0
259	Frontispiece: Air Electrode for the Lithium-Air Batteries: Materials and Structure Designs. ChemPlusChem, 2015, 80, .	1.3	0